

Melting behavior and growth of colquiriite laser crystals

D. Klimm*, R. Uecker, and P. Reiche

Institute for Crystal Growth, Max-Born-Str. 2, 12489 Berlin, Germany

Received 16 May 2004, accepted 30 July 2004

Published online 1 March 2005

Key words laser crystals, fluorides, hydrolysis, phase diagram.

PACS 42.55.Rz, 81.30.Dz, 81.10.–h

Colquiriite-type crystals like LiCaAlF_6 , LiSrAlF_6 , LiCaGaF_6 , and LiSrGaF_6 are interesting host crystals for Cr^{3+} or Ce^{3+} laser ion doping. Although the Ca compounds show interesting optical properties, the growth of these crystals is difficult due to incongruent melting. LiCaGaF_6 crystallizes with CaF_2 deficiency and melts incongruently at 710–720°C. Hydrolysis with traces of moisture is critical for all fluorides. AlF_3 and GaF_3 have the highest sensitivity among the main components of the colquiriites. Hydrolysis can only be slightly suppressed by hydrogen fluoride. Elementary fluorine or reactive gases as carbon tetrafluoride are more effective by several orders of magnitude.

© 2005 WILEY-VCH Verlag GmbH & Co. KGaA, Weinheim

1 Introduction

Viebahn [1] described some compounds with the general formula $\text{LiMe}^{\text{II}}\text{Me}^{\text{III}}\text{F}_6$ ($\text{Me}^{\text{II}} = \text{Ca, Sr, Cd}$; $\text{Me}^{\text{III}} = \text{Al, Ga, Ti, V, Cr, Fe}$), especially lithium calcium hexafluoroaluminate. Later this substance LiCaAlF_6 was found in the Bolivian tin mine Colquiri and this mineral was given the name Colquiriite after that location [2].

LiCaAlF_6 (LiCAF) [3], LiSrAlF_6 (LiSAF) [4], and LiSrGaF_6 (LiSGaF) [5] are used as host crystals for trivalent laser ions as Cr^{3+} and Ce^{3+} . Tuning ranges of the emission wavelength spanning several 100 nm are typical for such lasers. As the laser ions show broad-band absorption, diodes as well as flash lamps can be used for pumping. Reports on crystal growth and laser properties of LiCaGaF_6 (LiCGaF) are scarce.

Table 1 Optical and thermal properties of colquiriite crystals with Cr^{3+} doping [3,4,6,7].

Crystal	LiCaAlF_6	LiSrAlF_6	LiCaGaF_6	LiSrGaF_6
Emission peak (nm)	763	846	770	835
Tuning range (nm)	720...840	780...1000		780...920
Lifetime (μs)	170	67	200	88
Melting point (°C)	810	766	762	716
Thermal expansion (10^{-6}K^{-1})	$\alpha_{11} = 22.0$ $\alpha_{33} = 3.6$	$\alpha_{11} = 18.8$ $\alpha_{33} = -10$		$\alpha_{11} = 12$ $\alpha_{33} = 0$
Thermal conductivity ($\text{W}/(\text{K}\cdot\text{m})$)	$\lambda_{11} = 4.58$ $\lambda_{33} = 5.14$	$\lambda_{11} = 3.0$ $\lambda_{33} = 3.3$		$\lambda_{11} = 3.4$ $\lambda_{33} = 3.6$

The optical properties of colquiriites are interesting, but up to now these crystals are not very often used as laser hosts. Only Cr:LiSAF based fixed wavelength lasers of 430 nm and 442 nm (frequency doubled, *Melles Griot*) and Cr:LiSAF tuneable lasers (820...970 nm, *Rainbow Photonics*) are offered commercially [8]. Different reasons are responsible for the currently limited industrial application of colquiriite-type laser crystals:

* Corresponding author: e-mail: klimm@ikz-berlin.de

1. Cracking of the crystal can occur during growth and during laser action, as the thermal conductivity is low and the expansion is large and highly anisotropic (Table 1).
2. The vapour pressure of the components LiF, AlF₃, and GaF₃ at the melting point of the colquiriites is already high. Accordingly, evaporation of these components from the free melt surface can occur. Such incongruent evaporation shifts the melt composition and can lead to scattering centres that derogate crystal quality.
3. All fluorides are more or less sensitive to hydrolysis that may result from traces of water in the atmosphere or in the starting materials.

The first limitation is an intrinsic property of colquiriites as these crystals exhibit large $|\alpha_{11} - \alpha_{33}|$. Thermal stresses σ within nonlinear temperature fields are proportional to this term and cannot be avoided completely [9]. Nevertheless σ can often be kept within tolerable limits, if the geometrical dimension l of the crystals is small, as σ is proportionally l^2 . Moreover, $|\alpha_{11} - \alpha_{33}|$ is considerably smaller for LiSGaF as compared to LiSAF, thus leading to a higher thermal shock resistivity of the gallium compound.

The second limitation was discussed in detail in a previous paper [10]. Especially, the compound LiAlF₄ reaches a vapour pressure close to 100 Pa in the temperature range of the melting points of the colquiriites. (No data are available on the corresponding Ga compound.) The underestimation of the chemical composition shift by vaporization losses of volatile species can lead to the incorporation of inclusions in crystals. Even the determination of the ternary phase diagrams LiF–Me^{II}F₂–Me^{III}F₃ is sometimes not straightforward and was discussed already controversially [11]. This paper will present first results on the ternary system LiF–CaF₂–GaF₃.

The third limitation was discussed previously mainly for the dopant CrF₃ [9,10] on the basis of thermodynamic equilibrium calculations and mass spectrometric measurements. It is self-evident that the growth of any fluoride crystal must be performed under strict exclusion of water. This means that dry starting materials have to be molten in an atmosphere with as small humidity as possible. Often crucibles made of graphite or vitreous carbon are used instead of Pt crucibles, as excess carbon and water are in chemical equilibrium with carbon monoxide CO, carbon dioxide CO₂, hydrogen H₂ and methane CH₄. The chemical reactions:



remove water from the system, if the temperature dependent reaction rate is sufficient large. This is usually the case for temperatures $\mathcal{G} \geq 400 \dots 500^\circ\text{C}$. Table 2 shows remaining concentrations of water in argon, if the gas is in equilibrium with excess carbon. Instead of discussing the main reaction paths (1) separately, the equilibrium concentrations were calculated with a Gibbs free energy minimization program [12].

Table 2 Calculated molar concentration x of H₂O in Ar, if the gas is equilibrated with excess carbon. Total pressure 1 bar. Initial humidity $x_0 = 100 \text{ ppm} = 10^{-4}$ or $10 \text{ ppm} = 10^{-5}$, respectively.

\mathcal{G} (°C)	400	600	800	1000	1200	1400	1600
x (ppb) ($x_0=100 \text{ ppm}$)	4600	43	1.3	0.12	0.021	0.006	0.002
x (ppb) ($x_0=10 \text{ ppm}$)	89	0.43	0.01	0.001	2×10^{-4}	6×10^{-5}	2×10^{-5}

From the values given in Table 2 it is obvious that the efficiency of water removal rises drastically at high working temperatures and if the initial gas purity is already high. It will be shown in the following that the water concentrations that remain at the colquiriite fusing temperatures $\mathcal{G}_f \approx 800^\circ\text{C}$ (Table 1) even after complete equilibration with excess carbon ($x \approx 0.01 \dots 1 \text{ ppb}$) are too high to avoid hydrolysis completely.

2 Volatility and determination of phase diagrams

Under the conditions of the crystal growth of colquiriites, lithium is always monovalent (LiF), and the other end members are always Me^{II}F₂ or Me^{III}F₃, respectively. Therefore, ternary phase equilibria of the fluorides can

be considered instead of quaternary equilibria between the 3 metals and fluorine. The concentration triangle of Fig. 1 shows the 3 end members together with each 2 binary compounds on the $\text{LiF}-\text{Me}^{\text{III}}\text{F}_3$ and $\text{Me}^{\text{II}}\text{F}_2-\text{Me}^{\text{III}}\text{F}_3$ edges as filled circles. In contrast to Ca_2AlF_7 [13], Weil [14] recently reported that the formula $\text{Sr}_5\text{Al}_2\text{F}_{16}$ instead of Sr_2AlF_7 is more accurate. The colquiriite in the centre of the triangle is always the only ternary compound. $\text{Li}_3\text{Me}^{\text{III}}\text{F}_6$ is the only binary compound that is known to melt congruently for all relevant Me^{III} . Phase equilibrium studies are often performed on the sections S1 or S2. LiAlF_4 and GaAlF_4 do not melt congruently. Therefore, S2 is not a binary subsystem. SrAlF_5 melts congruently [15] and $\text{LiF}-\text{SrAlF}_5$ is a true binary subsystem, but due to the incongruent melting of the counterpart CaAlF_5 the section S1 $\text{LiF}-\text{CaAlF}_5$ is not binary [11].

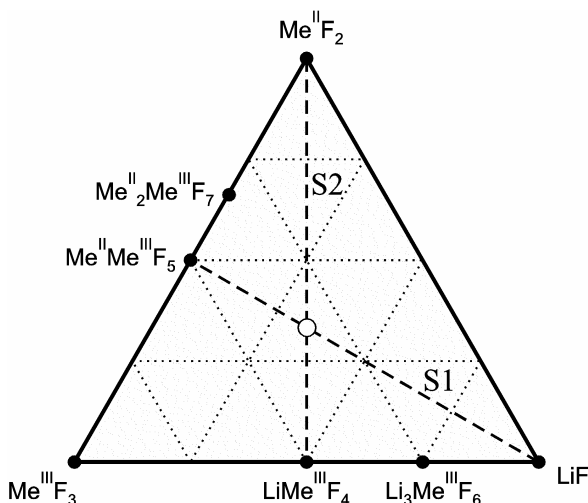


Fig. 1 Concentration triangle $\text{LiF}-\text{Me}^{\text{II}}\text{F}_2-\text{Me}^{\text{III}}\text{F}_3$ with quasi-binary compounds and the colquiriite composition (hollow circle) in the centre and the pseudo-binary sections S1 and S2 used for thermal analysis.

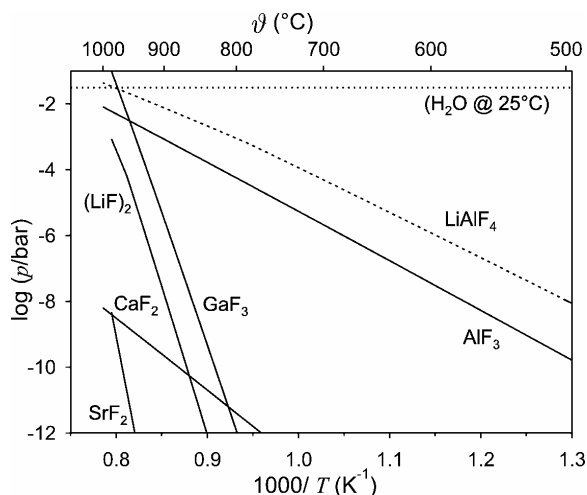


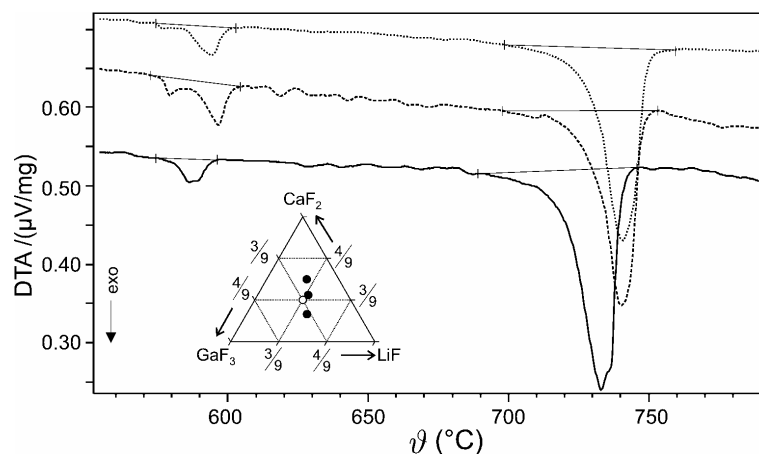
Fig. 2 Equilibrium partial pressure of the colquiriite basic components and of LiAlF_4 . $p_{\text{H}_2\text{O}}$ for constant $\theta=25^\circ\text{C}$ is marked for comparison.

The determination of phase equilibria is difficult for $\text{Me}^{\text{III}}\text{F}_3$ rich compositions due to the high vapour pressures p of GaF_3 , AlF_3 , and especially of the binary LiAlF_4 . Fig. 2 shows that p_{LiAlF_4} reaches in the melting temperature range of the colquiriites around 800°C almost 1 mbar, resulting in considerable evaporation losses, if no sealed DTA crucibles are used. Similar problems may arise during crystal growth from open crucibles and should be reduced by low axial temperature gradients that allow to maintain the overheating of the melt moderate.

The present thermoanalytic measurements were performed with a NETZSCH STA 409C equipped with a graphite furnace and a standard DTA/TG sample holder with Pt100%–Pt90%Rh10% thermocouples. Powdered LiF , CaF_2 and GaF_3 ($\geq 4\text{N}$ purity, 50...80 mg total sample mass) were weighed into graphite crucibles with lid. All measurements were performed in flowing (80 ml/min) 5N argon with heating/cooling rates of ± 10 K/min not higher than 50 K above the liquidus temperature. A first heating/cooling run was performed to homogenize the sample; data for the analysis were obtained from the subsequent second heating without prior opening the DTA furnace. If appropriate, extrapolated onsets were used as melting points. The TG signal was monitored to control evaporation losses and these were never found to exceed 0.6% of the sample mass during the whole thermal cycling process.

Pure GaF_3 (as AlF_3) does evaporate under ambient pressure without melting. The evaporation loss up to 830°C is 2%. Due to the composition shift by partial evaporation from $\text{Me}^{\text{III}}\text{F}_3$ rich compositions no DTA data on solidus and liquidus temperatures could be obtained in the left corner of the composition triangle (Fig. 1). Some data of the already published parts of the binary systems $\text{LiF}-\text{CaF}_2$ (see Ref. [17], Fig. 7491) and $\text{LiF}-\text{GaF}_3$ (see Ref. [17], Fig. 7493) are given in Table 3. A consistent description of the binary phase diagram $\text{CaF}_2-\text{GaF}_3$ could not be found. Two sharp endothermic peaks at 774 or 789°C in the heating curves were the main features and could be due to melting or phase transformations. Unfortunately, the liquidus usually could not be measured as evaporation from the DTA crucibles was too high for $\theta > 850^\circ\text{C}$.

Fig. 3 DTA heating curves for 3 mixtures close to the centre of the concentration triangle (Fig. 1) with compositions (from top to bottom, full circles) $\text{Li}_{0.945}\text{Ca}_{1.166}\text{Ga}_{0.889}\text{F}_{5.944}$ (dotted line), $\text{Li}_{1.018}\text{Ca}_{1.040}\text{Ga}_{0.942}\text{F}_{5.924}$ (dashed line), $\text{Li}_{1.087}\text{Ca}_{0.866}\text{Ga}_{1.027}\text{F}_{5.940}$ (full line). Hollow circle represents ideal composition LiCaGaF_6 .



Ten DTA measurements were performed with different powder mixtures around the nominal composition LiCaGaF_6 . Three second heating curves from such mixtures close to the centre of the concentration triangle are shown in Fig. 3. If LiCaGaF_6 has a congruent melting point, the line S1 in Fig. 1 between LiF and LiCaGaF_6 would separate partial triangles that are independent from each other. As the 3 compositions shown in Fig. 3 are situated above S1 (2 of them) or below S1 (1 of them), different ternary eutectic melting points should be expected. This is not the case. Instead the same melting temperature of residual eutectic $\approx 580^\circ\text{C}$ can be observed. As LiCaGaF_6 obviously does not span partial concentration triangles, incongruent melting of this compound at $710\dots 720^\circ\text{C}$ must be assumed. (The literature data in Table 1 give 716°C .) The ratio of the melting peak areas $\text{LiCaGaF}_6/\text{eutectic}$ is maximum for the lowermost data point shown in Fig. 3. A similar observation was reported for LiCaAlF_6 [16] where a true crystal composition $\text{LiCa}_{0.92}\text{AlF}_{5.84}$ was found. The stoichiometry deviation of $\text{LiCa}_{1-x}\text{GaF}_{6-2x}$ is in the same order of magnitude $x \approx 0.05\dots 0.08$. Unfortunately, single crystals could not be grown yet.

Table 3 Main thermodynamic features of binary subsystems between LiF, CaF_2 , and GaF_3 . Data that are confirmed in the present study are marked by an asterix.

subsystem	type	ϑ ($^\circ\text{C}$)	molar fractions [Li] - [Ca] - [Ga]	reference
LiF - CaF_2	simple eutectic	769	0.795-0.195-0.000	[17], Fig. 7491
LiF - GaF_3	congr. melting Li_3GaF_6	710*	0.750-0.000-0.250	[17], Fig. 7493
	phase transition Li_3GaF_6	525*		
	eutectic LiF- Li_3GaF_6	690*	0.820-0.000-0.180	
	eutectic Li_3GaF_6 - GaF_3	600	0.612-0.000-0.388	(this study 590°C)
CaF_2 - GaF_3	unidentified endothermal	774*	$[\text{CaF}_2] < 40\%$	
	unidentified endothermal	789*	$[\text{CaF}_2] > 10\%$	

3 Hydrolysis of fluorides

If heated in an atmosphere that contains moisture fluorides are subject to hydrolysis:



The degree of hydrolysis depends on the cation and on intensive system variables. It is obvious that the humidity of the system has to be reduced down to the lowest possible level to shift the equilibrium reaction to the left hand side. Growth chambers with low leakage rate, high purity gases and well dried starting materials (e.g. by moderate heating in vacuum) are inevitable.

Different ways are discussed to manage water traces remaining even after careful pre-treatment. Working with a large excess of HF in the growth atmosphere is one possibility to shift (2) to the fluoride side [18].

However, this shift is always incomplete, as the water is not removed from the system. The water can be removed to a large extent, if it reacts with suitable components that do not disturb crystal growth. The application of carbon instead of platinum as constructive material for crucible, thermal insulation and other components is only partially helpful for the colquiriites with comparably low melting point. The equilibrium constant k for $C + H_2O \leftrightarrow CO + H_2$ is $k_{800;1} = 7.7$ at 800°C and 1 bar. For fluorides with higher melting points (e.g. CaF_2 that melts at 1418°C) carbon is more effective: $k_{1418;1} = 1970$.

The oxidation of water by elementary fluorine (F_2 or F depending on partial pressure and \mathcal{G}) according $\text{H}_2\text{O} + \text{F}_2 \rightarrow 2 \text{HF} + \frac{1}{2} \text{O}_2$ is almost complete at room temperature and becomes only slightly worse up to the melting points of any fluoride. The treatment of substances with F_2 is not simple; but the alternative treatment with HF is not simple too. A previous paper [9] showed the efficient removal of water from the colquiriite dopant CrF_3 by treatment in F_2 at 300°C . Handling of fluorine becomes easier with XeF_2 . This white crystalline powder can be mixed with the starting materials and decomposes above 100°C to Xe and F_2 . The reactive atmosphere process proposed by Pastor in several articles [19-21] is an even easier effort to remove water during halide crystal growth. For this purpose solids or gases that provide free halide at elevated temperatures are added to the system. For fluoride crystal growth CF_4 was found to be very effective. Unfortunately, alkyl polyhalides are known to affect the earth's ozone layer and should be used with care. Table 4 compares the behaviour of the 3 component fluorides of LiCAF in different atmospheres containing 1 ppm residual water.

Table 4 Equilibrium activities a of some species at 800°C for heating of LiF , CaF_2 , and AlF_3 in different atmospheres (1 bar total pressure). All atmospheres are assumed to contain 1 ppm H_2O (1×10^{-6} = initial humidity).

fluoride	atmosphere	$a(\text{H}_2\text{O})$	$a(\text{HF})$	$a(\text{F})$	a (main hydrolysis product)
LiF	100% Ar	9.6×10^{-7}	4.3×10^{-8}	2.3×10^{-17}	0.21 ($\text{Li}_2\text{O}_{\text{sol}}$)
	100% HF	1×10^{-6}	1.0	3.7×10^{-10}	3.5×10^{-11} (LiOH_{liq})
	95%Ar+5% CF_4	1.6×10^{-25}	2.0×10^{-6}	3.7×10^{-9}	1.6×10^{-23} ($\text{Li}_2\text{O}_{\text{sol}}$)
CaF_2	100% Ar	9.1×10^{-7}	1.8×10^{-7}	9.7×10^{-17}	1.0 (CaO_{sol})
	100% HF	1×10^{-6}	1.0	3.7×10^{-10}	3.5×10^{-14} (CaO_{sol})
	95%Ar+5% CF_4	1.6×10^{-25}	2.0×10^{-6}	3.7×10^{-9}	1.4×10^{-21} (CaO_{sol})
AlF_3	100% Ar	3.8×10^{-12}	1.4×10^{-6}	1.3×10^{-17}	1.0 ($\alpha\text{-Al}_2\text{O}_3$)
	100% HF	7.4×10^{-7}	1.0	1.4×10^{-11}	2.7×10^{-7} ($\text{AlOF}_{2,\text{g}}$)
	95%Ar+5% CF_4	1.6×10^{-25}	2.0×10^{-6}	3.7×10^{-9}	3.4×10^{-12} ($\text{AlOF}_{2,\text{g}}$)

If CaF_2 or AlF_3 is heated in this slightly wet argon to the melting point of colquiriite, small amounts of CaO or $\alpha\text{-Al}_2\text{O}_3$, respectively, are formed by hydrolysis. LiF is more stable: Li_2O is not formed as condensed phase as its activity is <1 , but the value $a=0.21$ indicates that $\text{Li}_2\text{O}_{\text{sol}}$ is not far from formation as pure phase. If LiF or CaF_2 are heated in HF , the water content remains unchanged as no substantial hydrolysis occurs. Consequently, the activity of hydrolysis products (hydroxides and oxides) is very low ($a < 10^{-10}$). AlF_3 is considerably more sensitive and reduces the H_2O content of the atmosphere by $\approx 1/4$ under formation of gaseous aluminum oxide difluoride AlOF_2 [12,22]. If the fluorides are heated in Ar/CF_4 the CF_4 converts the water almost completely to HF and only negligible amounts of hydrolysis products can be formed.

Fig. 4 shows stability regions of different compounds of Li, Ca, and Al in dependence of humidity (abscissa) and the HF or F activity (= vapour pressure), respectively. The growth of optically clear LiCAF crystals will only be possible under conditions where all components are stable. This means that the growth has to be performed under conditions inside the top left "fluorides" region of the predominance diagrams. As the hydrolysis (2) is an equilibrium reaction, the formation of undesired products (usually oxides) starts already inside the "fluorides" region in the vicinity of the phase boundary.

HF is available either by thermolysis of potassium hydrogen fluoride $\text{KF}\cdot\text{HF}$, a hygroscopic powder offered commercially with only 99% purity [23] or as bottled gas with 99.95% purity and <100 ppm H_2O [24]. 100 ppm water correspond to $\log[p(\text{H}_2\text{O})/\text{bar}] = -4$, for this humidity the "fluorides" predominance region is limited at $\log[p(\text{HF})/\text{bar}] = -2$ (Fig. 4). Even working in pure hydrogen fluoride with 100 ppm humidity would result in an overcharging of only 2 orders of magnitude compared with the equilibrium value. Following (2) considerable amounts of hydrolysed fluoride must be expected. It is obvious from Fig. 4 that fluorine (as F or

F₂) is more effective by about 12 orders of magnitude for avoiding hydrolysis compared to HF. Table 3 shows that the small amounts of F that are in equilibrium with the "reactive gas" CF₄ are considerably more efficient than pure HF.

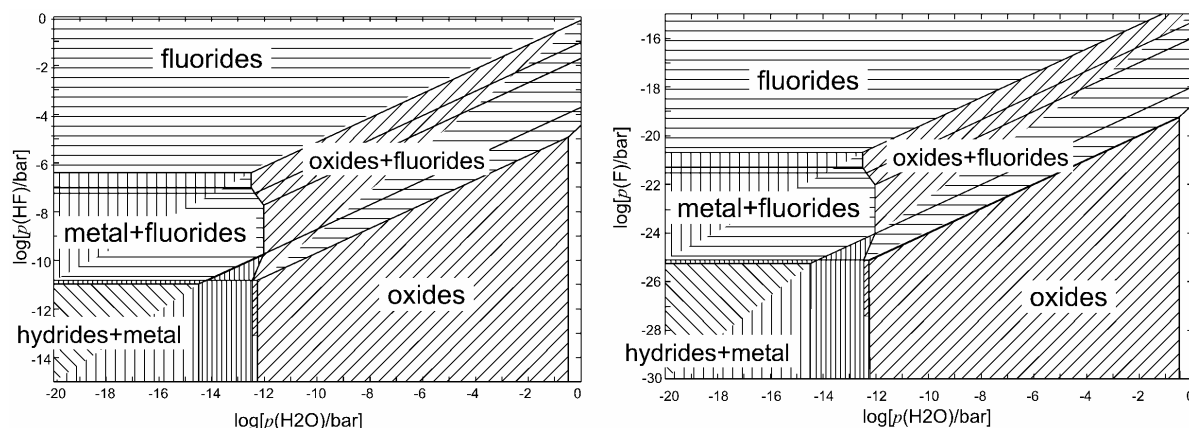


Fig. 4 Stability of compounds for the cations [Li]=[Ca]=[Al]= $\frac{1}{3}$ for different humidity (abscissa) dependent on HF fugacity (top) and F fugacity (bottom). The calculation [12] was done for $T=800^{\circ}\text{C}$ and $p = 1$ bar. Shadings: fluorides = horizontal, metals = vertical, hydrides = diagonal from top left, oxides = diagonal from bottom left. Narrow shadings = 3 types of phases stable. Small rectangles near $\log[p(\text{H}_2\text{O})/\text{bar}] = -12$ = oxides + metal (CaO+LiAlO₂+LiAl). Rectangle near $\log[p(\text{H}_2\text{O})/\text{bar}] = 0$ = CaO+LiAlO₂+LiOH.

4 Conclusions

The compounds LiCaAlF₆ (LiCAF) and LiCaGaF₆ (LiCGaF) have interesting optical parameters (e.g. lifetime, Table 1). Unfortunately the growth of both crystals is due to their incongruent melting more difficult as compared to the isotypic LiSrAlF₆ (LiSAF) and LiSrGaF₆ (LiSGaF) that melt congruently. As for all fluoride crystals, hydrolysis with traces of water coming from the starting materials or from the atmosphere is a major problem for crystal quality. It is necessary to perform the treatment of the materials and the crystal growth process under such conditions that allow exclusion of water as good as possible. Hydrolysis with remaining traces of humidity can only partially be avoided by hydrogen fluoride. Instead, treatment with elementary fluorine or with reactive gases as carbon tetrafluoride that supply fluorine at elevated temperature are more effective.

Acknowledgements The authors express their gratitude to S. Ganschow for fruitful collaboration.

References

- [1] W. Viebahn, Z. anorg. allg. Chem. **386**, 335 (1971).
- [2] K. Walenta, B. Lehmann, and M. Zwiener, Tscherma's Mineralog. Petrog. Mitt. **27**, 275 (1980).
- [3] S. A. Payne, L. L. Chase, H. W. Newkirk, L. K. Smith, and W. F. Krupke, IEEE J. Quantum Electron **24**, 2243 (1988).
- [4] S. A. Payne, L. L. Chase, L. K. Smith, W. L. Kway, and H. W. Newkirk, J. Appl. Phys. **66**, 1051 (1989).
- [5] L. K. Smith, S. A. Payne, W. L. Kway, L. L. Chase, and B. H. T. Chai, IEEE J. Quantum Electron. **28**, 2612 (1992).
- [6] A. Cassanho and H. Jenssen, Laser Focus World, May 1997.
- [7] B. W. Woods, S. A. Payne, J. E. Marion, R. S. Hughes, and L. E. Davis, J. Opt. Soc. Am. B **8**, 970 (1991).
- [8] T. A. Samtleben and J. Hulliger, Optics and Lasers in Engineering, **43**, 252 (2005).
- [9] D. Klimm, G. Lacayo, and P. Reiche, J. Cryst. Growth **210**, 683 (2000).
- [10] D. Klimm and P. Reiche, Cryst. Res. Technol. **34**, 145 (1999).
- [11] D. Klimm and P. Reiche, J. Cryst. Growth **249**, 388 (2003).
- [12] FactSage 5.2, <http://www.factsage.com/> (GTT Technologies, Kaiserstr. 100, 52134 Herzogenrath, Germany, 2003).
- [13] R. Domesle and R. Hoppe, Z. Kristallogr. **153**, 317 (1980).

- [14] M. Weil, *Z. Anorg. Allg. Chem.* **627**, 2669 (2001).
- [15] J. P. Meehan and E. J. Wilson, *J. Cryst. Growth* **15**, 141 (1972).
- [16] D. Klimm and P. Reiche, *Cryst. Res. Technol.* **33**, 409 (1998).
- [17] L. P. Cook and H. F. McMurdie (Eds.), "Phase Diagrams for Ceramists, Vol. VII", The American Ceramic Society, 1989.
- [18] A. M. E. Santo, S. L. Baldochi, and S. P. Morato, *J. Cryst. Growth* **198/199**, 466 (1999).
- [19] R. C. Pastor, *J. Cryst. Growth* **200**, 510 (1999).
- [20] R. C. Pastor, *J. Cryst. Growth* **203**, 421 (1999).
- [21] R. C. Pastor, *J. Cryst. Growth* **207**, 102 (1999).
- [22] O. M. Uy, R. D. Srivastava, and M. Farber, *High Temp. Sci.* **4**, 227 (1972).
- [23] <http://www.alfa.com/> (item #11557).
- [24] <http://www.airliquide.com/>.